Title Page

Title:

Bimodal dynamics of granular organelles in primary renin-expressing cells revealed using TIRF microscopy

Running Head:

Imaging granule organelle dynamics in renin cells

Corresponding Author:

Charlotte Buckley [1]

cbuckley@exseed.ed.ac.uk

Other Authors:
Alison Dun [2]
Audrey Peter [1]
Christopher Bellamy[3]
Kenneth W. Gross [4]
Rory Duncan [2]
John J. Mullins [1]

Institutes:

1. BHF/University Centre for Cardiovascular Science
   University of Edinburgh
   Queen's Medical Research Institute
   47 Little France Crescent
   Edinburgh
   EH16 4TJ

2. Edinburgh Super Resolution Imaging Consortium
   Heriot-Watt University
   Riccarton Campus
   Edinburgh
   EH14 4AS
3. Department of Pathology
   Royal Infirmary of Edinburgh
   51 Little France Crescent
   Edinburgh
   EH16 4SA
4. Department of Molecular and Cellular Biology
   Roswell Park Cancer Institute
   Buffalo
   New York 14263

Abstract

Renin is the initiator and rate-limiting factor in the renin-angiotensin blood pressure regulation system. Whilst renin is not exclusively produced in the kidney, in non-murine species the synthesis and secretion of the active circulatory enzyme is confined almost exclusively to the dense core granules of juxtaglomerular (JG) cells, where prorenin is processed and stored for release via a regulated pathway. Despite its importance, the structural organization and regulation of granules within these cells is not well understood, in part due to the difficulty in culturing primary JG cells *in vitro* and the lack of appropriate cell lines.

We have streamlined the isolation and culture of primary renin-expressing cells suitable for high-speed, high-resolution live imaging using a Percoll gradient-based procedure to purify cells from RenGFP^{+} transgenic mice. Fibronectin-coated glass coverslips proved optimal for the adhesion of renin-expressing cells and facilitated live cell imaging at the plasma membrane of primary renin cells using total internal reflection fluorescence microscopy (TIRFM). To obtain quantitative data on intracellular function, we stained mixed granule and lysosome populations with Lysotracker Red and stimulated cells using 100 nM isoproterenol. Analysis of membrane-proximal acidic granular organelle dynamics and behavior within renin-expressing cells revealed the existence of two populations of granular organelles with distinct functional responses following isoproterenol stimulation. The application of high-resolution techniques for imaging JG and other specialized kidney cells provides new opportunities for investigating renal cell biology.

Keywords

Juxtaglomerular; TIRFM; granule tracking; renin

Abbreviations

TIRFM: total internal reflection fluorescence microscopy

JG: Juxtaglomerular

JGA: juxtaglomerular apparatus

SNR: Signal-to-noise ratio

ACEi: Angiotensin converting enzyme inhibitor

MIP: Maximum intensity projection

FACS: Fluorescence activated cell sorting

Introduction

Renin is the rate-limiting enzyme in the renin angiotensin system, a key regulator of mammalian blood pressure. Under normal physiological conditions the synthesis and secretion of active renin is confined to the juxtaglomerular (JG) cells of the renal juxtaglomerular apparatus (JGA). Here it is packaged into dense core storage granules for stimulated release in the regulated secretory pathway (21,45) through the generation of cAMP (16,22,29).

The paradigm of the JG cell has changed dramatically in recent years. Cells of renin lineage have displayed novel rolls as progenitor cells within the JGA, for example contributing to the generation of mesangium (23), parietal epithelial cells of the Bowman's capsule (44) and podocytes (31,44). Furthermore, JG cells have also been shown to facilitate the secretion of other factors in addition to renin. In their seminal paper, Brunskill *et al.* (5) compared gene expression profiles of renin cells at different stages of development, showing that several angiogenic factors are also secreted. These factors were suggested to provide cues for wide ranging purposes such as cell-to-cell communication, endothelial elongation and matrix digestion. The fact that these cells play a key role in JGA tissue remodeling and secrete factors for wide ranging purposes indicate that process of secretion from renin-expressing cells may be more complex than originally thought.

Parallels have also been drawn between renin-containing granules and lysosomes. JG cell granules co-localise with key lysosomal membrane proteins LIMP2 (30,49) and LAMP1 (30), and lysosomal enzymes β-glucuronidase (18), acid phosphatase (54) and cathepsins B, H, L (32,50,51). Correct segmentation of renin granules requires the presence of lysosomal trafficking regulator (Lyst) (24). Unlike the majority of granules in secretory cell types, renin granules have autophagic abilities, taking up exogenous tracers such as cationized ferritin and horseradish peroxidases in a lysosomal manner (54). Granules acquire phosphomannosyl residues (14), the recognition markers for mannose-6-phospate receptors which mediate enzyme targeting to lysosomes. It has also been confirmed that lysosomal hydrolysis can process prorenin accurately (59). This wide body of evidence strongly suggests that JG dense-core renin granules are modified lysosomes.

Relatively little is known about the onset of granulation, or the mechanism of secretion via such lysosomal granules. Despite apparent exocytosis, no evidence has been published to date showing granule motion in JG cells. The lack of information is due in part to the difficulty in performing high-resolution intracellular imaging of these cells. Cultured primary JG cells only synthesize renin and respond to cAMP-mediated renin release for approximately 48-72 hours (10). Since they represent 0.001-0.01% of the viable kidney cell population (5), equating to approximately 1000 cells per kidney digest, a large number of kidney digests must be pooled and Fluorescence Activated Cell Sorting (FACS)-sorted to obtain a homogeneous population of JG cells, exposing the sensitive JG cells to extended and relatively harsh environmental conditions (room temperature and atmospheric CO_2). This is compounded when multiple populations of

cells are required for experimental duplicates. Alternatively, Percoll gradients have been used as an effective means of enriching for JG cells and shortening the extraction process when homogeneous populations of cells are not required (8,38,41). Whilst the AS4.1 immortalized cell line is frequently used in lieu of primary renin-expressing cells, the cAMP renin-release pathway is maximally-stimulated in these (25), making them unsuitable for granule secretion-based studies. Renin-GFP reporter mice (26) allow the rapid identification of JG cells, enable their analysis using FACS, and provide a convenient marker for the identification of *bona fide* JG cells for microscopy.

The development of high-speed image acquisition has enabled highly accurate granule tracking in real time under controlled conditions. One such technique is Total Internal Reflection Fluorescence Microscopy (TIRFM) in which the excitation laser light is introduced at a critical angle whereby it is totally internally reflected at the coverslip/aqueous medium interface. At this angle very little excitation energy enters the cell and, instead, an evanescent electromagnetic wave is generated at the surface of the coverslip. This field decays exponentially, and thus only propagates a few hundred nm into the sample. Therefore only fluorophores within this thin optical section are excited, eliminating out-of-focus light from the majority of the cell and improving axial resolution and signal-to-noise ratio (SNR). TIRFM has been used extensively to investigate granular motion at the cellular membrane (13,47).

We have modified the standard isolation protocol for the efficient isolation and culture of renin-expressing cells suitable for high resolution optical microscopy and describe the application of TIRFM, together with high-speed imaging to reveal novel dynamics of acidic granular organelles in renin-expressing cells.

Methods

Animals and pharmacological treatment:

Experiments were conducted in accordance with the Animals (Scientific Procedures) Act 1986, under local ethical guidelines. Adult RenGFP$^{+/-}$ mice (26) were used throughout the study. Captopril (1mg/ml) was administered in the drinking water for 7 days prior to cell extraction.

Cell isolation & culture:

Animals were sacrificed by cervical dislocation, the kidneys dissected, decapsulated and placed in ice cold DMEM (10% FCS). Kidneys were finely diced, the homogenate transferred to digestion buffer (DMEM, 1mg/ml, collagenase I, II, IV; ThermoFisher) and incubated in a shaking waterbath (30-45 mins, 37^{o}C, 150

rpm), titurating every 15 mins. Digestion was stopped using DMEM and filtered sequentially through 100 µm and 70 µm filters. Cells were pelleted (140g, 8 mins), the supernatant discarded and the pellet resuspended in DMEM (10% FCS). A Percoll (Sigma, P1644) gradient was created in DMEM (10% FCS) by layering 5 ml each of 50%, 40%, 30%, 20%, 10% Percoll, using phenol red in alternate layers. Resuspended cells were then applied to the top of the gradient and centrifuged (HB6 rotor, Sorvall RCPlus centrifuge, 27,000 g, swing-out rotor, 4^{o}C, 30 mins). The discontinuous Percoll gradient used produced 5 distinct layers; for each layer, the cells were cultured and imaged to determine which layer the GFP-positive cells were found in (the 30% layer). Cells were removed from these layers using a sterile Pasteur pipette, discarding the layers containing low density fragments of cells and the blood cells. This pooled subset was pelleted, resuspended in DMEM (10% FCS, 1X Pen/Strep) and filtered through a 40µm filter. Primary renin cells were cultured in pre-warmed phenol-free primary culture medium (37^{o}C, 5% CO_2) for less than 24 hours for tracking experiments, and for less than 48 hours for staining experiments.

25mm diameter coverslips were immersed in 0.1 M NaOH/0.1% Decon-90 solution, dH_2O, 100% ethanol, 100% acetone and 1L dH_2O sequentially. Coverslips were placed in either fibronectin (Sigma, F1141) or PDL (Sigma, P6407) at 50 µg/ml for 1 hr with gentle agitation. These were placed in 6-well dishes, with the heterogeneous population of isolated cells plated at an approximate density of $0.5x10^6$ cells/cm^2.

Renin and α-smooth muscle actin staining:

Cells were fixed for 20mins in 4% (w/v) PFA, washed twice with PBS, incubated in 50mM NH_4Cl (10mins) and rewashed. A 5% (v/v) goat serum blocking (1hr) was performed, followed by incubation overnight (4^{o}C) with an anti-renin antibody (rabbit anti mouse; (48)) or an α-smooth muscle actin antibody (mouse anti mouse, 1:100, Sigma A2547). After washing, a 1hr incubation in goat anti-rabbit AF-555 (Life Technologies, A-21428) was followed by further washes (3x5mins). Coverslips were air-dried, Prolong Gold antifade mountant with added DAPI was placed in the coverslip center and placed on a glass slide (overnight, room temperature). Nail varnish was applied to the edge of the coverslip for affixation and the slides stored at 4^{o}C.

Renin induction protocol, RNA extraction, cDNA generation and quantitative PCR:

Primary cells were allowed to adhere overnight, the FCS-free medium applied to the wells for 24 hours prior to induction. Medium was replaced with 2ml FCS-free DMEM containing 10µM forskolin (Cell signaling, 38285) and 100µM IBMX (Sigma, I7018) for a further 24 hours. Cells were then washed with PBS and Trizol (Ambion, 15596018) added to each well, titurating well to lyse cells and incubating for 5 mins.

A phenol chloroform extraction was performed to extract RNA. In brief, chloroform was added and the mixture shaken vigorously and centrifuged (10,000*g*, 4^{o}C, 15 mins). The upper, aqueous phase was added to isopropanol, mixed thoroughly, incubated for 10mins (4^{o}C) and centrifuged (8,400*g,* 5 mins). The

supernatant was removed and the pellet air dried and resuspended in RNAse-free water. Contaminating genomic DNA was removed through the use of a DNAFree Kit (Ambion, AM1906), following the product guidelines. cDNA was performed using a High Capacity cDNA Reverse Transcription kit (Applied Biosciences, 4368814), following the product guidelines and using a Thermocycler (Applied Biosciences, Veriti 96-well).

The Roche Universal Probe Library was used for quantitative PCR. 25ng/µl cDNA was used per reaction, with triplicates performed. Each reaction contained 5µl LightCycler 480 Probes Master 2X mastermix (Roche, 04 887 301 001), 0.1µl primer pairs (20µM, Eurofins Genomic EU) and 0.1µl the relevant probe (100nM) and 2.8µl RNAse-free water and 2µl cDNA. 18S was used as a housekeeping gene. 18S Primers/Probe: F – ctcaacacgggaaacctcac; R – cgctccaccaactaagaacg; 97. Renin Primers/Probe: F – cccgacatttcctttgacc; R – tgtgcacagcttgtctctcc; 16. Reactions were run on a Roche Lightcycler 480 at 95^{o}C (15mins), then 95^{o}C for 10s, 60^{o}C for 30s, 72oC for 1s, repeated 50 times. Automated Cp value identification was performed using Roche Lightcycler software.

Flow Cytometry:

Cells were isolated as above, but were resuspended in sorting medium (PBS, 2% FCS), filtered through a 40 µm strainer and placed in a suspended beam on a FACS ARIA II cytometer and analyzed on FACSDiva c6.0 with appropriate gating set using GFP$^{-/-}$ control kidneys.

Microscopy techniques:

Epifluorescence: A Nikon (Eclipse Ti; Nikon Instruments) with a mercury arc lamp (X-cit 120 series, Lumen dynamics) light source in fluorescence mode with DAPI (Ex: 350nm/50 nm; Em: 470/40 nm) and FITC (Ex: 470/40 nm, Em: 525/50 nm) filters was used for DAPI and GFP image acquisition, respectively. A 60X (1.4 N.A. Plan Apo) or 40X (1.3 NA Plan Fluor oil) objective lens was used.

Live cell imaging was performed on an Olympus Cell Excellence IX81 using a 150X (1.45 NA) oil immersion objective lens combined with a Hamamatsu EMCCD camera, operated through the Xcellence advanced live cell imaging software package at constant EM gain in the linear range. A temperature controlled block stage with CO_2 integration ensured cells remained at 37^{o}C and 5% (v/v) CO_2. 100 mW diode lasers providing excitation at 405nm, 491nm and 561nm were used for data acquisition in both widefield and TIRFM modes, coupled independently in a fiber combiner. 100 nM Lysotracker Red DND-99 (Molecular Probes) was added to the culture medium 30 mins prior to image data acquisition. Acidic granular organelles loaded with Lysotracker were imaged at 14 Hz for 70s using the 561 nm laser line in widefield mode. For TIRFM, the angle of the laser was increased and focused towards the coverslip. TIRF was reached when fluorescence from the acidic granular organelles further than a few hundred nm from the cell membrane were no longer visible. The non-specific β-adrenergic agonist Isoproterenol (1) was used at

concentrations similar to those in the literature (100 nM) (20). Therefore culture media containing isoproterenol (100 nM) was added to the perfusion chamber after 35s of acquisition (via a syringe with a meter length of tubing) and further images acquired. Image acquisition occurred continuously throughout baseline, addition of isoproterenol and after addition.

Image analysis:

Tracking was performed using Imaris 7.7 (Bitplane) tracking module via spot creation (starting diameters: 700 nm for large acidic granular organelles, 300nm for small organelles; spots were detected through and tracked using the Brownian model. Tracks were eliminated from analysis if tracking was lost for > 70 – 140 ms. Instantaneous speed, average speed, track length and displacement were extracted for each organelle. The diameter was quantified in ImageJ by manually measuring the diameter 3 times and averaging. Two conditions were analyzed per cell for data collected using widefield microscopy: baseline and isoproterenol treated. Four conditions were analyzed for data collected using TIRFM: baseline motion, isoproterenol administration, 35s and 70s post-treatment. Acidic granular organelles were included for mean speed analysis if they were tracked over the entire duration they remained within the field of view. Only organelles tracked over the full time course were included in analysis of track-length travelled and displacement (displacement is the as-the-crow-flies start-to-end distance in the image). Images are presented as maximum intensity projections (MIP), generated using Fiji.

Statistical analysis:

Data are presented as the mean +/- S.E.M. Statistical significance was tested with a one way Anova using the non-parametric Kruskal-Wallis test with Dunn post hoc analysis. *: $p<0.05$; **: $p<0.01$; ***:$p<0.001$; ****: $p<0.0001$.

Results

To enable easy identification, renin-expressing cells were isolated from RenGFP$^+$ mice. To optimize the extraction and culture protocol it was essential that the maximum number of RenGFP$^+$ cells possible were isolated, therefore renin expression was induced by pre-treatment of animals with the ACE inhibitor, captopril (1 mg/ml, 7 days). The increase in RenGFP$^+$ cell number was verified using flow cytometry where, on average, the number of GFP$^+$ cells increased from 0.02 +/- 0/01% (untreated) to 0.22 +/- 0.02% ($p=0.0002$) after captopril treatment (Fig 1 a-c). This 10-fold increase was sufficient to allow rapid location of GFP-positive cells using the 150X magnification lens required for live, high resolution imaging.

Renin-expressing cells isolated using a Percoll gradient were cultured for 24 hours on either PDL- (Fig 1e) or fibronectin-coated (Fig 1d) coverslips to compare adherence efficiency. All renin cells visualized remained 'balled-up' on PDL-coated dishes, but adhered much more efficiently to fibronectin-coated dishes, where the majority of renin-expressing cells showed rapid, full adhesion. This was therefore selected as the most appropriate for culture of isolated renin-expressing cells. Granular renin expression within GFP-expressing primary cells was confirmed using immunocytochemistry with an anti-renin antibody (Fig 2a-c). Staining for α-smooth muscle actin showed that the isolated cells were of a smooth muscle origin (Fig 2d-f), with actin filaments seen to run along the edge of the cells. To ensure that these cells responded appropriately to cAMP stimulation, cells underwent a renin induction protocol where IBMX and forskolin stimulated renin expression. Upon stimulation, renin expression levels increased significantly by ~11-fold when compared to controls (Fig 2g, $p=0.00008$).

Intracellular acidic granular organelles were identified using Lysotracker Red, as previously published (13,42). Once renin cells were identified on the basis of their GFP expression, two-channel images were acquired using widefield microscopy for each cell to ensure that the collected Lysotracker signal was from renin-expressing cells (Fig 3, top panel). Granular organelles were imaged over time and characterized as 'large' ($d>500$nm) or 'small' ($d<500$ nm). A number of large acidic granular organelles moved appreciably in response to isoproterenol treatment (Fig 3a,c white arrows). Whilst the large acidic granules exhibited motion around a restricted location (caged, Fig 3, green arrows), small granular organelles moved much greater distances in a directed motion (Fig 3, yellow arrows). This is visually demonstrated using MIPs (Fig 3b,d) and tracks (Fig 3g-j), and can be seen dynamically in Supplementary Videos 1 and 2.

Tracking these structures using widefield microscopy showed that the speed of large granular organelles was significantly increased from 340 (+/-10) nm/s to 590 (+/-30) nm/s ($p < 0.0001$) after addition of isoproterenol (Fig 3f). Due to low SNR when acquiring using widefield microscopy, tracks from smaller acidic organelles were not acquired.

Under TIRFM illumination, Lysotracker-labelled granular organelles were imaged using the oblique angle of the TIRF laser to increase the SNR. Qualitative assessment of tracking fidelity was performed by

comparing Lysotracker signal to GFP location, and the analyzed tracks to MIPs over time (Fig 4 a-l). As expected, both caged and tethered motion of large granular organelles was observed. Specific examples of movement are more clearly visualized in Fig 4 (d-l), where motion from a sub-cellular region is demonstrated with a MIP and the Imaris track. Examples of motion in response to isoproterenol treatment are shown for large (Fig 4d-i) and small (Fig 4j-l) granular organelles.

By using TIRFM both large and small granular structures were tracked, with each individual diameter measured in ImageJ. Plotting the diameter against mean speed revealed two distinct populations of acidic granular organelles: large granular structures showed a constrained range of speeds which rarely exceeded 1 μm/s (Fig 5 a) and small granular structures, which exhibited a more diverse range of speeds from 0.25 μm/s to 2.37 μm/s.

The large granular organelles responded dynamically to the addition of isoproterenol, showing significant increase in mean speed and track length (Fig 5 b-g), indicating that we may be seeing a regulated dynamic response to stimulus known to promote renin secretion. These speeds, averaged over the 50-80 measured tracks, are in keeping with the speeds measured for the individual tracks.

Conversely, although the average speed of the small granular organelles showed an acute increase during addition of the isoproterenol, this decreased back to baseline (Fig 5b-d). It is particularly striking that addition of isoproterenol had no significant effect on track length.

Discussion

We present a novel methodology for quantitative high-resolution intracellular imaging of primary renin-expressing cells and show evidence of intracellular acid granular organelle motion within live renin cells. Tracking was used to demonstrate the potential of the system for acquiring quantitative information regarding organelle behavior.

By adapting the well-established use of Percoll gradients to isolate fluorescent renin-expressing cells (9,10,34,38,39,41) and adapting cell culture conditions we were able to acquire detailed images of freshly isolated renin-expressing cells. The use of a discontinuous multi-layered Percoll gradient and the simple expedient of using phenol red to distinguish alternate layers speeded up the extraction process.

Despite PDL being used previously for the culture of JG cells, it was not optimal in our studies. Primary renin-expressing cells failed to adhere fully to PDL-coated culture dishes and exhibited a 'balled-up' appearance similar to that observed in other studies (11,34,35,38,39,41). Fibronectin was significantly more effective at allowing rapid adhesion of primary renin cells to the culture dish; no instances of full adherence were seen from cells plated on PDL over many experiments. Fibronectin is known to contribute to the extracellular matrix of the JGA, where it is localized to the distal end of the afferent arteriole within the ECM (6), whereas PDL is a positively charged amino acid polymer which acts as an adherence factor. This suggests that factors provided by the ECM are better suited to efficient adherence of primary renin-expressing cells.

The use of IBMX and forskolin is a well-established method of assessing whether renin-producing cells are responding appropriately to cAMP stimulation (11,20,34). IBMX inhibits phosphodiesterases, which are known to inhibit renin transcription and stimulation through the breakdown of cAMP to 5'AMP (40). Forskolin directly activates adenylyl cyclases 5 and 6, stimulating renin transcription and secretion (11,38). The 11-fold increase in gene expression seen in our primary cultured renin-expressing cells is similar to previous reports (11), indicating that the primary cultured renin-expressing cells responds appropriately to cAMP stimulation such as the chosen stimulus isoproterenol, a β-adrenergic agonist acting through the cAMP stimulation pathway (Aldheni, 2011).

In the absence of fluorescent reporter-renin fusion lines of mice, the ease and rapidity of accumulation of acidotropic dyes within granules and lysosomes and their strong fluorescent signals make them particularly well suited to the identification of acidic granular organelle and high speed acquisition live imaging. The low pH within early granules (pH 4 – 6) is achieved through the action of intracellular H^+-ATPases which catalyze the transmembrane exchange of protons and aid aggregation of the granule core (33,55), and this low pH that allows the identification of granular structures by such acidotropic dyes. Classically quinacrine has been the acidic dye of choice and it has been shown to bind with high affinity to granules within JG cells, having been used as an intravital stain both in fixed samples (2,7), in microperfused JGA preparations

(42,43) and in multiphoton imaging in live mice. Since GFP and quinacrine have similar excitation/emission spectra, a similar acidotropic dye, Lysotracker red was chosen for the current study. This dye has previously been used to label large dense core vesicles in live cultured secretory cells (13) and in live JG cells as part of an isolated perfused JGA preparation (27,58). Although Lysotracker, like quinacrine, does not specifically co-localize with renin, it is a well-recognized method of identifying renin-containing dense core granules within renin cells. Although technically challenging due to the low pH present in granules, the development of renin-fusion proteins that would label granules directly would be an advantage and may distinguish between the population of renin granules and the resident lysosomal compartment.

To date, relatively little research has been conducted on granule transport in JG cells due to the technical challenges involved. By combining our isolation and culture technique with high resolution widefield and TIRF microscopy, we successfully visualized the motion of intracellular acidic lysosomal granular compartments in renin cells for the first time. Even though TIRF was used to visualize membrane-proximal lysosomal organelles, acidic granular organelles of diameters of over 1μm were visualized. This could be indicative of irregularly shaped organelles, such as those seen when performing 3D reconstructions of EM-fixed JG cells (52). Peti-Peterdi *et al* (43) reported dimming and disappearance of fluorescence from individual quinacrine-loaded granules in response to 100 μM isoproterenol perfusion in JGA preparations, but no associated granule trafficking. This could be attributed to the difference in acquisition rate; in their study images were collected every 10s for 10 mins or 1 image/0.8s using confocal light scanning microscopy whereas in the present study images were acquired every 70ms thereby enabling the dynamics to be observed.

When acquiring data in TIRF mode, granular translation in z caused a dimming of fluorescence intensity, however this was not considered an exocytotic event. When an acidified granule fuses with the plasma membrane, the granule interior will immediately equilibrate with the extracellular fluid at approximately pH7.4. By using a pH-sensitive dye, this increase in pH from acidic to neutral would cause a flash of fluorescence as the dye leaves the granule interior (36). Even following the addition of isoproterenol no bursts of fluorescence associated with exocytosis were observed in our primary renin-expressing cells. Exocytotic events in JG cells are notoriously difficult to visualize and the only evidence to date comes from electron microscopy studies in which exocytosis was stimulated by an acute decrease in kidney perfusion pressure (46) and from isolated kidneys perfused with both isoproterenol (10nM) and the Ca^{2+}-chelating agent EGTA (52). Patch clamp studies of individual, primary, cultured JG cells showed that under baseline conditions only 0.9 +/- 0.1% total renin content was released per hour, and that stimulation with 10μM isoproterenol increased the exocytosis rate to 40 +/-5% per hour (15). Therefore it is likely that the stimulation given in this study was not sufficient, or viewed for long enough, to elicit and detect exocytotic events. Future studies will investigate the effects of isoproterenol administration on renin secretion.

There is a particularly marked difference in the dynamic parameters of the two pools of granular compartments identified; the small vesicle structures (d<500nm) are significantly faster and, presumably as a consequence, travel a much longer track length and displacement than large structures. These pools also respond independently to the addition of isoproterenol. It is known that under an acute stimulus, increased secretion of active renin ensues, whereas under chronic stimulation a concomitant increase in both prorenin and active renin is seen in the circulation (57). Since the large granular organelles respond in a regulated fashion to the acute stimulus whilst the smaller do not, it suggests that measurement of dynamic parameters allows different pools of acidic granular organelles on different regulatory pathways to be distinguished.

Very little research on granule transport has been performed in JG cells. Granules and vesicles are transported around cells by motor proteins on either microtubules or actin filaments; motor proteins are known to drive long range transport whilst actin-based motors tether cargo proteins, however the interaction between the two remains unclear (28). Ogawa *et al.* reported the presence of actin filaments on electron-dense granules within JG cells, and that when actin was disrupted using Cytochalasin B the granules moved closer to the membrane (37). Whilst both precursor and mature versions of renin have been shown to bind to microtubules (12), no staining for them has been performed. However it is clear from the present study that active organelle transport is important within renin-expressing cells. Although it is possible that organelle diffusion is taking place, it is unlikely to be the only transport mechanism; instantaneous diffusion has been shown to transport vesicles at approximately 10-15 nm/s (3), a speed too low to account for many of the organelle speeds measured. The two most common motor proteins are kinesin and dynein; dynein transports vesicles along microtubules at velocities of ~800-1000 nm/s (56), whilst kinesin only facilitates movement of up to ~600nm/s (53). It is therefore possible that the larger organelles are being transported via kinesin motors, whilst dynein motors are responsible for transport of smaller vesicles.

To increase the number of renin cells, we isolated cells from animals treated with an ACEi for 7 days, a well-documented method of increasing renin cell numbers through the stimulation of afferent arteriole vascular smooth muscle cells towards a renin-expressing phenotype (19). Whilst it is therefore probable that there is heterogeneity in the differentiation state of the GFP-positive, renin-expressing cell population, it has been shown in the literature (Glenn, 2008) and via antibody staining in this paper, that these cells express renin. Renin-expressing cells are well documented as possessing smooth muscle cell characteristics; bioinformatics analysis of JG cells by Brunskill *et al* (5) revealed that fully differentiated JG cells retain both smooth muscle and renin phenotypes, driven and maintained by unique transcriptional networks to allow endocrine and contractile function. Recruited renin-expressing cells have also been shown to develop large, electron-dense renin-containing granules (4,46). Therefore it would be valuable to extend the use of TIRFM to investigate comparative granule/organelle dynamics in fully-differentiated and induced renin cells.

The ability to image dynamic processes within JG cells is crucial if we are to further our understanding of granulopoiesis and secretory mechanisms. Using the experimental design outlined in this paper, it may be possible to investigate the mechanisms of different signaling pathways for renin secretion and the activity of renin cells under different types of physiological stress.

Acknowledgements

The authors thank the facility staff for animal husbandry and Dr Linda Mullins for technical and manuscript discussion.

Grants

This work was financially supported by a British Heart Foundation Centre of Research Excellence award, and CB was the recipient of a 4-year BHF PhD studentship. We acknowledge the support of the Society for Endocrinology for an Early Career Award for CB, and the MRC, BBSRC and EPSERC for funding of the ESRIC facilities.

References

(1) Aldehni, F., Tang, T., Madsen, K., Plattner, M., Schreiber, A., Friis, U.G., Hammond, H.K., Han, P.L. and Schweda, F., Stimulation of renin secretion by catecholamines is dependent on adenylyl cyclases 5 and 6.*Hypertension*, *57*(3), pp.460-468, 2011.

(2) Ålund, M., Juxtaglomerular cell activity during hemorrhage and ischemia as revealed by quinacrine histofluorescence. *Acta Physiologica Scandinavica*, *110*(2), pp.113-121, 1980

(3) Aschenbrenner, L., Naccache, S.N. and Hasson, T., Uncoated endocytic vesicles require the unconventional myosin, Myo6, for rapid transport through actin barriers. *Molecular biology of the cell*, *15*(5), pp.2253-2263, 2004

(4) Berka, J.L., Alcorn, D., Ryan, G.B. and Skinner, S.L., Renin processing studied by immunogold localization of prorenin and renin in granular juxtaglomerular cells in mice treated with enalapril. *Cell and tissue research*, *268*(1), pp.141-148, 1992

(5) Brunskill, E. W., Sequeira-Lopez, M. L. S., Pentz, E. S., Lin, E., Yu, J., Aronow, B. J., Potter, S.S., Gomez, R. A. Genes that confer the identity of the renin cell. *Journal of the American Society of Nephrology*, *22*(12),2213-2225, 2011

(6) Blanc-Brunat, N., Mutin, M. and Peyrol, S., Immunohistochemical localization of type IV collagen fibronectin and laminin in the juxtaglomerular apparatus of the rat kidney. *Cellular and molecular biology*, *35*(4), pp.469-484, 1988

(7) Casellas, D, Dupont, M., Kaskel, F.J., Inagami, T. and Moore, L.C., Direct visualization of renin-cell distribution in preglomerular vascular trees dissected from rat kidney. *American Journal of Physiology-Renal Physiology*, *265*(1), pp.F151-F156, 1993

(8) Chen, L., Kim, S. M., Oppermann, M., Faulhaber-Walter, R., Huang, Y., Mizel, D., Chen, M., Lopez, M.L.S., Weinstein, L.S., Gomez, R.A. and Briggs, J. P., Regulation of renin in mice with Cre recombinase-mediated deletion of G protein Gsα in juxtaglomerular cells. *American Journal of Physiology-Renal Physiology*, *292*(1), F27-F37, 2007

(9) Della Bruna, R., Pinet, F., Corvol, P. and Kurtz, A., Regulation of renin secretion and renin synthesis by second messengers in isolated mouse juxtaglomerular cells. *Cellular Physiology and Biochemistry*, *1*(2), pp.98-110, 1991

(10) Della Bruna, R., Pinet, F, Corvol, P. and Kurtz, A., Calmodulin antagonists stimulate renin secretion and inhibit renin synthesis in vitro. *American Journal of Physiology-Renal Physiology*, *262*(3), pp.F397-F402, 1992

(11) Della Bruna, R., Pinet, F., Corvol, P. and Kurtz, A., Regulation of renin secretion and renin synthesis by second messengers in isolated mouse juxtaglomerular cells. *Cellular Physiology and Biochemistry*, *1*(2), pp.98-110, 1993

(12) Dicou, E. and Brachet, P., Precursors of the nerve growth factor γ subunit and renin bind to microtubules. *European Journal of Biochemistry*,*143*(2), pp.381-387, 1984

(13) Duncan, R.R., Greaves, J., Wiegand, U.K., Matskevich, I., Bodammer, G., Apps, D.K., Shipston, M.J. and Chow, R.H., Functional and spatial segregation of secretory vesicle pools according to vesicle age. *Nature*,*422*(6928), pp.176-180, 2003

(14) Faust, P.L., Chirgwin, J.M. and Kornfeld, S., Renin, a secretory glycoprotein, acquires phosphomannosyl residues. *The Journal of cell biology*, *105*(5), pp.1947-1955, 1987

(15) Friis, U.G., Jensen, B.L., Aas, J.K. and Skøtt, O., Direct demonstration of exocytosis and endocytosis in single mouse juxtaglomerular cells. *Circulation research*, *84*(8), pp.929-936, 1999

(16) Friis, U.G., Jensen, B.L., Sethi, S., Andreasen, D., Hansen, P.B. and Skøtt, O., Control of renin secretion from rat juxtaglomerular cells by cAMP-specific phosphodiesterases. *Circulation research*, *90*(9), pp.996-1003, 2002

(17) Friis, U.G., Madsen, K., Svenningsen, P., Hansen, P.B., Gulaveerasingam, A., Jørgensen, F., Aalkjær, C., Skøtt, O. and Jensen, B.L., Hypotonicity-induced Renin exocytosis from juxtaglomerular cells requires aquaporin-1 and cyclooxygenase-2. *Journal of the American Society of Nephrology*, *20*(10), pp.2154-2161, 2009

(18) Gomba, S. and Soltész, B.M., Histochemistry of lysosomal enzymes in juxtaglomerular cells. *Experientia*, *25*(5), pp.513-513, 1969

(19) Gomez, R.A., Lynch, K.R., Chevalier, R.L., Everett, A.D., Johns, D.W., Wilfong, N.E.Y.S.A., Peach, M.J. and Carey, R.M., Renin and angiotensinogen gene expression and intrarenal renin distribution during ACE inhibition. *American Journal of Physiology-Renal Physiology*, *254*(6), pp.F900-F906, 1988

(20) Grünberger, C., Obermayer, B., Klar, J., Kurtz, A. and Schweda, F., The Calcium Paradoxon of Renin Release Calcium Suppresses Renin Exocytosis by Inhibition of Calcium-Dependent Adenylate Cyclases AC5 and AC6. *Circulation research*, *99*(11), pp.1197-1206, 2006

(21) Hackenthal, E.M.D.R., Paul, M., Ganten, D. and Taugner, R., Morphology, physiology, and molecular biology of renin secretion.*Physiological reviews*, *70*(4), pp.1067-1116, 1990

(22) Holmer, S.R., Kaissling, B., Putnik, K., Pfeifer, M., Krämer, B.K., Riegger, G.A. and Kurtz, A., Beta-adrenergic stimulation of renin expression in vivo. *Journal of hypertension*, *15*(12), pp.1471-1479, 1997

(23) Hugo, C., Shankland, S.J., Bowen-Pope, D.F., Couser, W.G. and Johnson, R.J., Extraglomerular origin of the mesangial cell after injury. A new role of the juxtaglomerular apparatus. *Journal of Clinical Investigation*,*100*(4), p.786, 1997

(24) Jensen, B. L., Rasch, R., Nyengaard, J. R., & Skøtt, O., Giant renin secretory granules in beige mouse renal afferent arterioles. *Cell and tissue research*, *288*(2), 399-406, 1997

(25) Jones, C.A., Petrovic, N., Novak, E.K., Swank, R.T., Sigmund, C.D. and Gross, K.W., Biosynthesis of renin in mouse kidney tumor As4. 1 cells. *European Journal of Biochemistry*, *243*(1-2), pp.181-190, 1997

(26) Jones, C.A., Hurley, M.I., Black, T.A., Kane, C.M., Pan, L., Pruitt, S.C. and Gross, K.W., Expression of a renin/GFP transgene in mouse embryonic, extra-embryonic, and adult tissues. *Physiological genomics*,*4*(1), pp.75-81, 2000

(27) Kang, J.J., Toma, I., Sipos, A., McCulloch, F. and Peti-Peterdi, J., Quantitative imaging of basic functions in renal (patho) physiology.*American Journal of Physiology-Renal Physiology*, *291*(2), pp.F495-F502, 2006

(28) Kapitein, L.C., van Bergeijk, P., Lipka, J., Keijzer, N., Wulf, P.S., Katrukha, E.A., Akhmanova, A. and Hoogenraad, C.C., Myosin-V opposes microtubule-based cargo transport and drives directional motility on cortical actin. *Current Biology*, *23*(9), pp.828-834, 2013

(29) Kim, S.M., Chen, L., Faulhaber-Walter, R., Oppermann, M., Huang, Y., Mizel, D., Briggs, J.P. and Schnermann, J., Regulation of renin secretion and expression in mice deficient in β1-and β2-adrenergic receptors.*Hypertension*, *50*(1), pp.103-109, 2007

(30) Lee, D., Desmond, M.J., Fraser, S.A., Katerelos, M., Gleich, K., Berkovic, S.F. and Power, D.A., Expression of the transmembrane lysosomal protein SCARB2/Limp-2 in renin secretory granules controls renin release. *Nephron Experimental Nephrology*, *122*(3-4), pp.103-113, 2013

(31)Lichtnekert, J., Kaverina, N.V., Eng, D.G., Gross, K.W., Kutz, J.N., Pippin, J.W. and Shankland, S.J., Renin-Angiotensin-Aldosterone System Inhibition Increases Podocyte Derivation from Cells of Renin Lineage.*Journal of the American Society of Nephrology*, pp.ASN-2015080877, 2016

(32) Matsuba, H, Watanabe, T, Watanabe, M, Ishii, Y, Waguri, S, Kominami, E and Uchiyama, Y, Immunocytochemical localization of prorenin, renin, and cathepsins B, H, and L in juxtaglomerular cells of rat kidney. *Journal of Histochemistry & Cytochemistry*, *37*(11), pp.1689-1697, 1989

(33) Mellman, I., Fuchs, R. and Helenius, A., Acidification of the endocytic and exocytic pathways. *Annual review of biochemistry*, *55*(1), pp.663-700, 1986

(34) Mendez, M., Gross, K.W., Glenn, S.T., Garvin, J.L. and Carretero, O.A., Vesicle-associated membrane protein-2 (VAMP2) mediates cAMP-stimulated renin release in mouse juxtaglomerular cells. *Journal of Biological Chemistry*, *286*(32), pp.28608-28618, 2011

(35) Mendez, M. and Gaisano, H.Y., Role of the SNARE protein SNAP23 on cAMP-stimulated renin release in mouse juxtaglomerular cells.*American Journal of Physiology-Renal Physiology*, *304*(5), pp.F498-F504, 2013

(36) Miesenböck, G., De Angelis, D.A. and Rothman, J.E. Visualizing secretion and synaptic transmission with pH-sensitive green fluorescent proteins. *Nature*, *394*(6689), pp.192-195, 1998

(37) Ogawa, K., Yamasato, M. and Taniguchi, K., Exocytosis of secretory granules in the juxtaglomerular granular cells of kidneys. *The Anatomical Record*, *243*(3), pp.336-346, 1995

(38) Ortiz-Capisano, M. C., Ortiz, P. A., Harding, P., Garvin, J. L., & Beierwaltes, W. H., Adenylyl cyclase isoform v mediates renin release from juxtaglomerular cells. *Hypertension*, *49*(3), 618-624, 2007a

(39) Ortiz-Capisano, M.C., Ortiz, P.A., Harding, P., Garvin, J.L. and Beierwaltes, W.H., Decreased intracellular calcium stimulates renin release via calcium-inhibitable adenylyl cyclase. *Hypertension*, *49*(1), pp.162-169, 2007b

(40) Ortiz-Capisano, M.C., Liao, T.D., Ortiz, P.A. and Beierwaltes, W.H., Calcium-dependent phosphodiesterase 1C inhibits renin release from isolated juxtaglomerular cells. *American Journal of Physiology-Regulatory, Integrative and Comparative Physiology*, *297*(5), pp.R1469-R1476, 2009

(41) Ortiz-Capisano, M. C., Reddy, M., Mendez, M., Garvin, J. L., & Beierwaltes, W. H., Juxtaglomerular cell CaSR stimulation decreases renin release via activation of the PLC/IP3 pathway and the ryanodine receptor.*American Journal of Physiology-Renal Physiology*, *304*(3), F248-F256, 2013

(42) Peti-Peterdi, J., Fintha, A., Fuson, A.L., Tousson, A. and Chow, R.H., Real-time imaging of renin release in vitro. *American Journal of Physiology-Renal Physiology*, *287*(2), pp.F329-F335, 2004

(43) Peti-Peterdi, J., Multiphoton imaging of renal tissues in vitro.*American Journal of Physiology-Renal Physiology*, *288*(6), pp.F1079-F1083, 2005.

(44) Pippin, J.W., Sparks, M.A., Glenn, S.T., Buitrago, S., Coffman, T.M., Duffield, J.S., Gross, K.W. and Shankland, S.J., Cells of renin lineage are progenitors of podocytes and parietal epithelial cells in experimental glomerular disease. *The American journal of pathology*, *183*(2), pp.542-557, 2013

(45) Pratt, R.E., Carleton, J.E., Richie, J.P., Heusser, C. and Dzau, V.J., Human renin biosynthesis and secretion in normal and ischemic kidneys.*Proceedings of the National Academy of Sciences*, *84*(22), pp.7837-7840, 1987

(46) Rasch, R., Jensen, B.L., Nyengaard, J.R. and Skøtt, O., Quantitative changes in rat renin secretory granules after acute and chronic stimulation of the renin system. *Cell and tissue research*, *292*(3), pp.563-571, 1998

(47) Ravier, M.A., Tsuboi, T. and Rutter, G.A., Imaging a target of Ca 2+ signalling: dense core granule exocytosis viewed by total internal reflection fluorescence microscopy. *Methods*, *46*(3), pp.233-238, 2008

(48) Rohrwasser, A., Morgan, T., Dillon, H.F., Zhao, L., Callaway, C.W., Hillas, E., Zhang, S., Cheng, T., Inagami, T., Ward, K. and Terreros, D.A., Elements of a paracrine tubular renin- angiotensin system along the entire nephron. *Hypertension*, *34*(6), pp.1265-1274, 1999

(49) Schmid, J., Oelbe, M., Saftig, P., Schwake, M. and Schweda, F., Parallel regulation of renin and lysosomal integral membrane protein 2 in renin-producing cells: further evidence for a lysosomal nature of renin secretory vesicles. *Pflügers Archiv-European Journal of Physiology*,*465*(6), pp.895-905, 2013

(50) Shinagawa, T., Nakayama, K., Uchiyama, Y., Kominami, E., Doi, Y., Hashiba, K., Yano, K., Hsueh, W.A. and Murakami, K., Role of cathepsin B as prorenin processing enzyme in human kidney. *Hypertension Research*, *18*(2), pp.131-136, 1995

(51) Soltesz, B. M., Gomba, S., & Szokol, M., Lysosomal enzymes in the juxtaglomerular cell granules. *Experientia*, *35*(4), 533-534, 1979

(52) Steppan, D., Zügner, A., Rachel, R. and Kurtz, A., Structural analysis suggests that renin is released by compound exocytosis. *Kidney international*, *83*(2), pp.233-241, 2013

(53) Svoboda, K. and Block, S.M., Force and velocity measured for single kinesin molecules. *Cell*, *77*(5), pp.773-784, 1994

(54) Taugner, R., Whalley, A., Angermüller, S., Bührle, C.P. and Hackenthal, E., Are the renin-containing granules of juxtaglomerular epithelioid cells modified lysosomes?. *Cell and tissue research*, *239*(3), pp.575-587, 1985

(55) Taugner, R. and Metz, R., Development and fate of the secretory granules of juxtaglomerular epithelioid cells. *Cell and tissue research*,*246*(3), pp.595-606, 1986

(56) Toba, S., Watanabe, T.M., Yamaguchi-Okimoto, L., Toyoshima, Y.Y. and Higuchi, H., Overlapping hand-over-hand mechanism of single molecular motility of cytoplasmic dynein. *Proceedings of the National Academy of Sciences*, *103*(15), pp.5741-5745, 2006

(57) Toffelmire, E.B., Slater, K., Corvol, P., Menard, J. and Schambelan, M., Response of plasma prorenin and active renin to chronic and acute alterations of renin secretion in normal humans. Studies using a direct immunoradiometric assay. *Journal of Clinical Investigation*, *83*(2), p.679, 1989

(58) Vargas, S.L., Toma, I., Kang, J.J., Meer, E.J. and Peti-Peterdi, J., Activation of the succinate receptor GPR91 in macula densa cells causes renin release. *Journal of the American Society of Nephrology*, *20*(5), pp.1002-1011, 2009

(59) Xa, L.K., Lacombe, M.J., Mercure, C., Lazure, C. and Reudelhuber, T.L., General lysosomal hydrolysis can process prorenin accurately.*American Journal of Physiology-Regulatory, Integrative and Comparative Physiology*, *307*(5), pp.R505-R513, 2014

Figure Legends

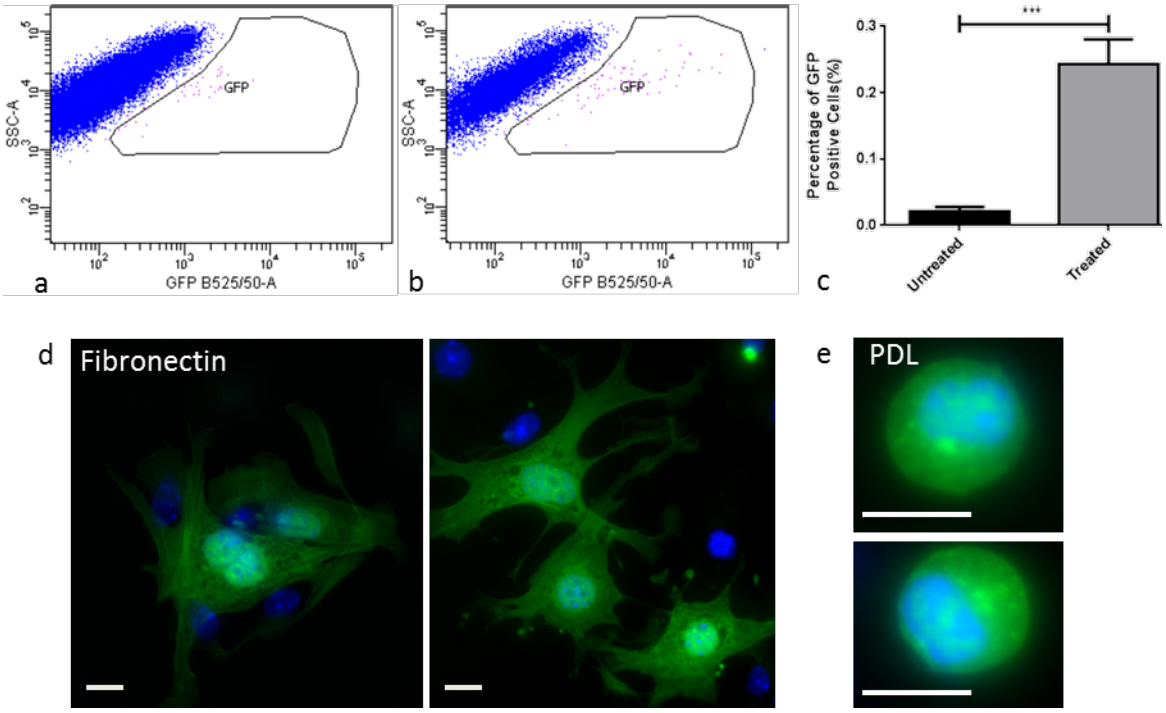

Figure 1: Representative plots from flow cytometry analysis of RenGFP$^{+/-}$ kidney digests (a) at baseline and (b) after captopril treatment (1 mg/ml, 7 days). (c) The average increase in GFP-positive cell number measured using flow cytometry (n=3, 5 respectively). (d-e) Adherence of primary RenGFP$^{+/-}$ renin cells (green) isolated from captopril treated RenGFP$^{+/-}$ kidney digests using a Percoll gradient and plated on coverslips coated with 50 µg/ml (d) fibronectin or (e) PDL, fixed with 4% PFA and stained with DAPI (blue).

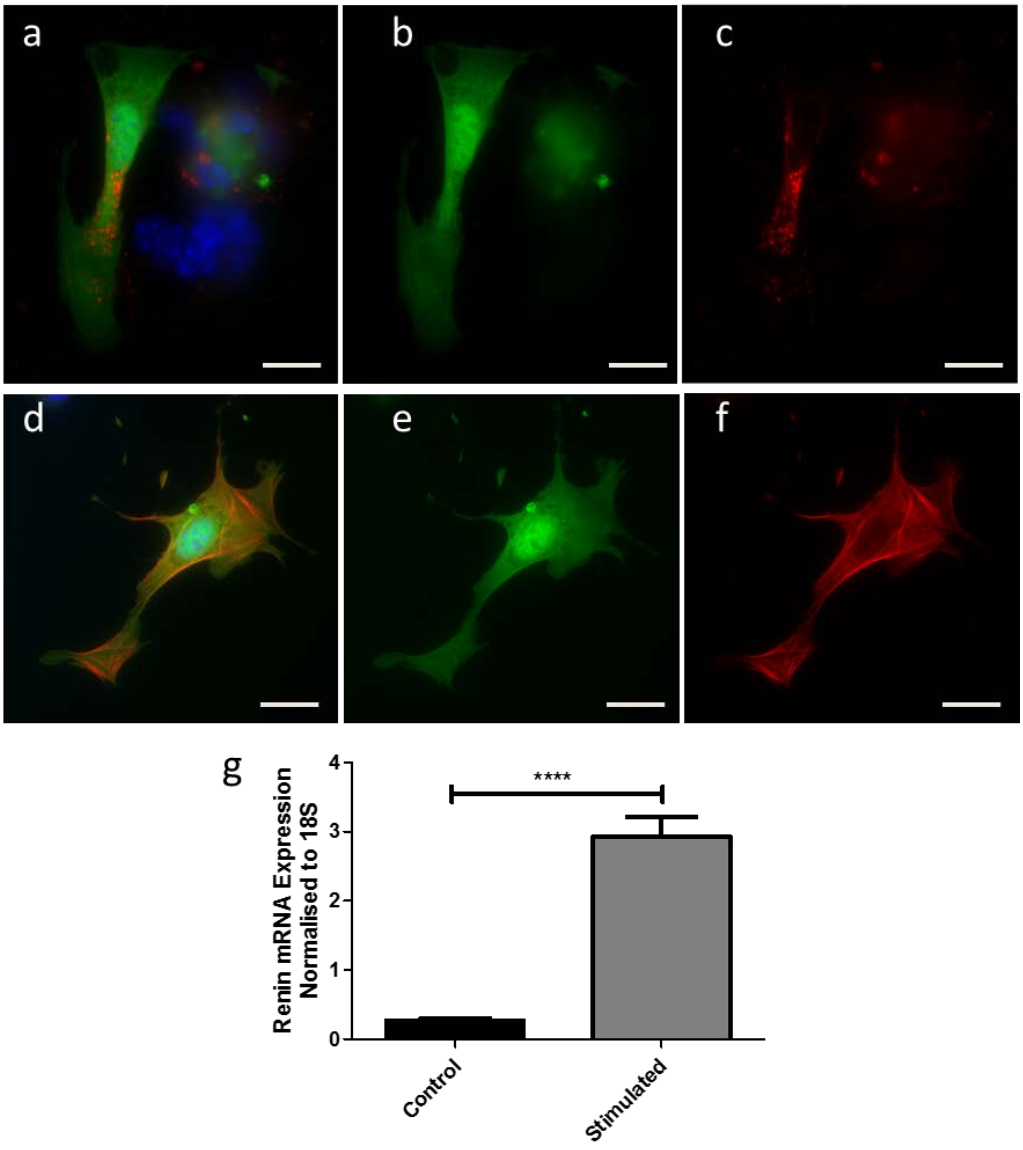

Figure 2: Characterization of primary renin cells cultured on fibronectin. Cells were isolated from captopril-treated RenGFP$^{+/-}$ kidney digests and cultured on coverslips coated with fibronectin (50 µg/ml) for 24 hours and fixed with 4% PFA. (a-c) Renin expression in GFP-positive cells (green) was confirmed using an anti-renin antibody (red) and stained with DAPI (blue), shown in the final merged image. (d-f) Renin cells (green) were also stained for α-smooth muscle actin (red). All scale bars represent 20 µm. (g) Renin gene expression in primary renin cells, under baseline or stimulated conditions (100µM IBMX, 10µM forskolin for 24hrs, n=3). Error bars represent S.E.M., Student t-test performed, **** indicates $p<0.0001$.

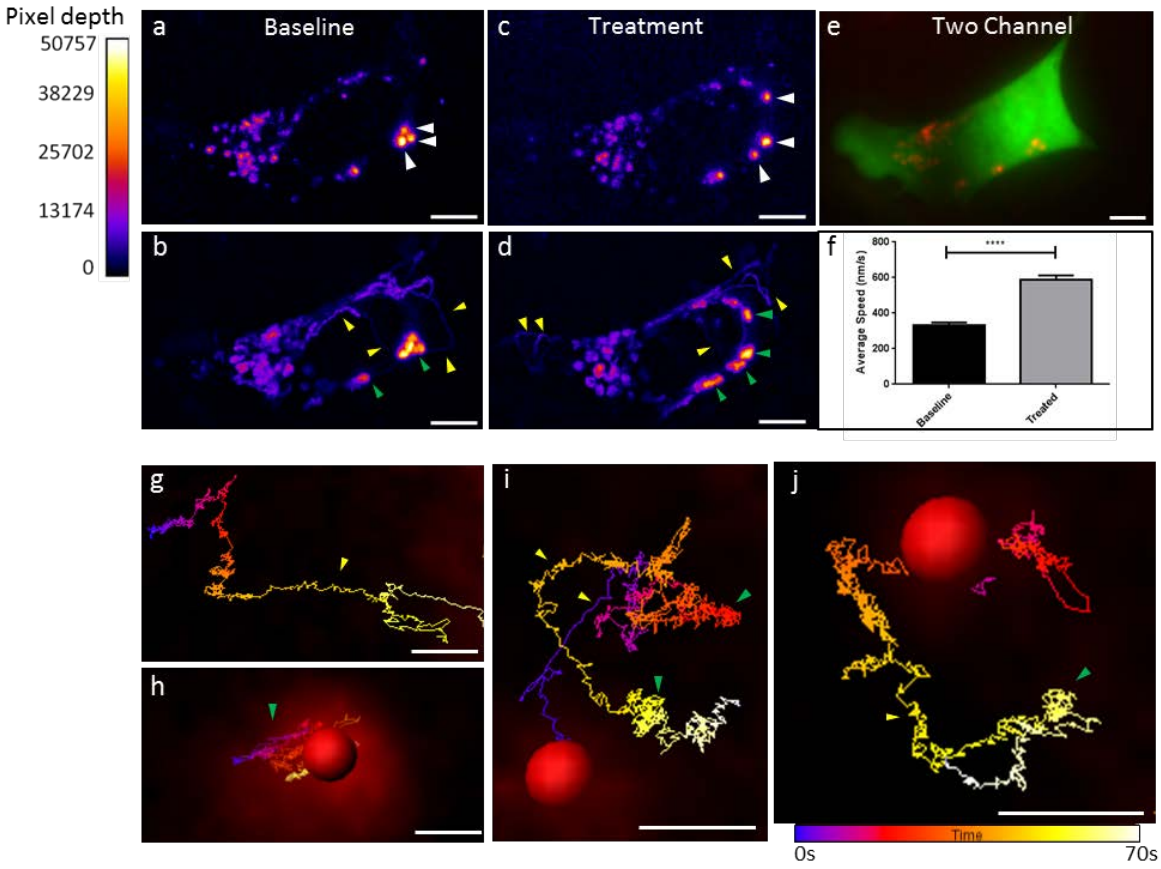

Figure 3: Widefield microscopy analysis of acidic granular organelle dynamics. (a-f) Renin cells from RenGFP^{+} kidneys were stained with Lysotracker (100 nM) and identified on the basis of GFP signal using widefield microscopy. (e) Merged images verified that the Lysotracker signal acquired was from within RenGFP^{+} cells. Lysotracker signal acquired at (a, b) baseline and (c, d) after treatment with isoproterenol (100 nM) is shown using a ramp scale showing intensity from low to high (scale bar of bit depth shown) for enhanced contrast, presented as (a, c) a single frame or (b, d) a MIP across 70s of image acquisition. White arrows: examples of large acidic granular organelle which moved appreciably in response to isoproterenol; yellow arrows: directed motion; green arrows: tethered motion. Scale bars represent 5 μm (f) Average speed of tracking data from large (d > 500 nm) granules. Data are S.E.M. **** indicates $p < 0.0001$. (g-j) Examples of individual acidic granular organelle motion of large organelles (d>500 nm) within the cells shown in (a-e). Tracks are superimposed onto raw Lysotracker signal intensity data. Track color correlated

with time (color bar time scale below images represents 0 – 70s). Yellow arrows indicate examples of directed motion; green arrows represent examples of caged motion. Scale bars represent 0.5 µm.

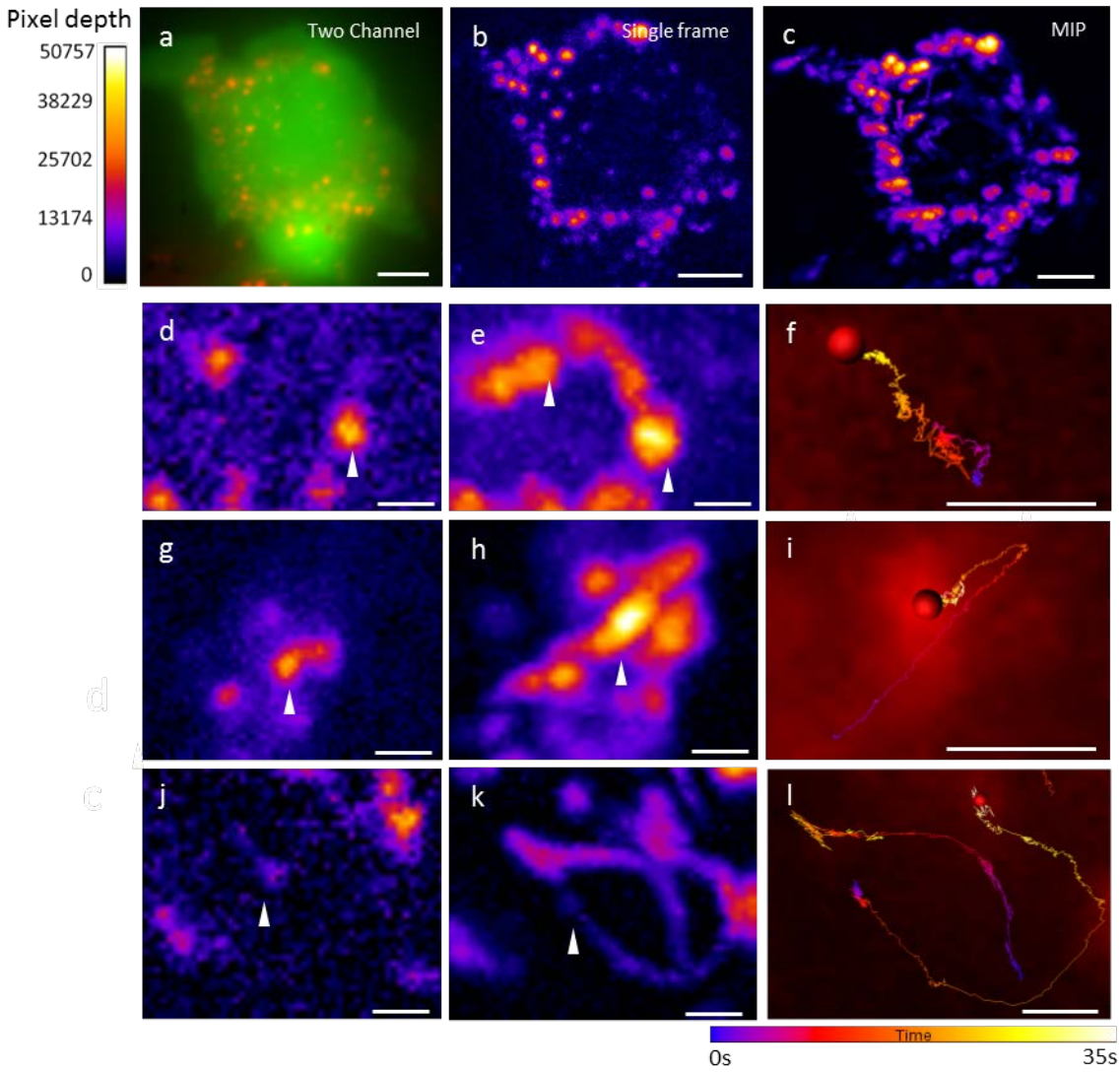

Figure 4: TIRFM analysis of acidic granular organelle dynamics. (a-c): (a) Renin cells were identified on the basis of their GFP expression (green) and loaded with 100 nM Lysotracker (red). (b) Exemplary single frame taken during addition of isoproterenol. (c) The time course is represented as a MIP over 140 s. Large (d>500nm) and small (d<500nm) granules were tracked separately. Scale bars represent 5 µm. (d-l) Examples of individual organelle motion, with (d,g,j) a single frame, (e,h,k) the MIP and (f,i,l) the corresponding Imaris tracks shown. Images are visualized using a ramp scale showing intensity from low

to high (scale bar of bit depth shown). White arrows indicate the acidic granular organelle of interest. Track color correlates with time (from blue at the start to yellow at the end, as indicated in the legend) Scale bars represent 1 μm.

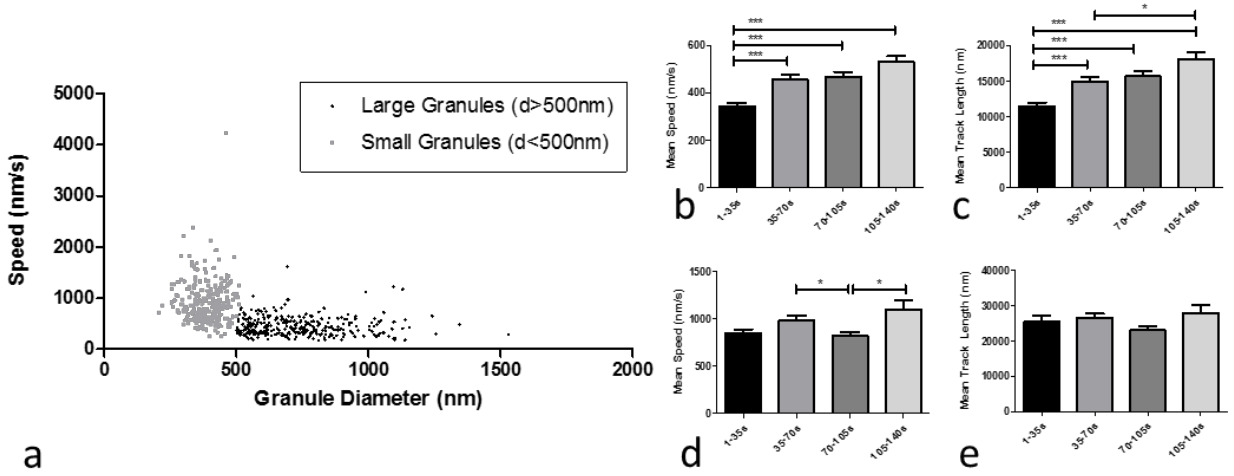

Figure 5: (a) Distribution of organelle sizes and speeds in primary renin cells, imaged using TIRFM. The diameter of each granule tracked was measured in ImageJ prior to being tracked. A 500 nm granule diameter was used to distinguish between large (black) and small (light grey) acidic granular organelles. (b,c) Large (d>500nm) and (d,e) small (d<500nm) organelles were tracked separately at baseline (1-35s), during addition of isoproterenol (35-70s), and after treatment (70-105s, 105-140s; 70ms/frame). (b,d) Mean speed and (c,e) track length were extracted. 3 cells were analyzed, with on average 77 large and 60 small organelles tracked per condition. A one-way Anova using the non-parametric Kruskal-Wallis test with Dunn post hoc analysis was performed.